

Article ID: 1006-8775(2016) S1-0067-11

HAZE-TO-FOG TRANSFORMATION DURING A LONG LASTING, LOW VISIBILITY EPISODE IN NANJING

ZHANG Shu-ting (张舒婷), NIU Sheng-jie (牛生杰)

(Key Laboratory of Meteorological Disaster, Ministry of Education / Joint International Research Laboratory of Climate and Environment Change / Collaborative Innovation Center on Forecast and Evaluation of Meteorological Disasters, Nanjing University of Information Science and Technology, Nanjing 210044 China)

Abstract: Haze-to-fog transformation during a long lasting, low visibility episode was examined using the observations from a comprehensive field campaign conducted in Nanjing, China during 4-9 December 2013. In this episode, haze was transformed into fog and the fog lasted for dozens of hours. The impacts of meteorological factors such as wind, temperature (T) and relative humidity (RH) on haze, transition and fog during this episode were investigated. Results revealed significant differences between haze and fog days, due to their different formation mechanisms. Comparison was made for boundary-layer conditions during hazy days, haze-to-fog days and foggy days. Distributions of wind speed and wind direction as well as synoptic weather conditions around Nanjing had determinative impacts on the occurrences and characteristics of haze and fog. Weakened southerly wind in southern Nanjing resulted in high concentration of pollutants, and haze events occurred frequently during the study period. The wind speed was less than 1 m s^{-1} in the haze event, which resulted in a stable atmospheric condition and weak dispersion of the pollutants. The height of the temperature inversion was about 400 m during the period. The inversion intensity was weak and the temperature-difference was 4°C km^{-1} or less in haze, while the inversion was stronger, and temperature-difference was about 6°C km^{-1} , approaching the inversion layer intensity in the fog event. Haze event is strongly influenced by ambient RH. RH values increased, which resulted in haze days evidently increased, suggesting that an increasing fraction of haze events be caused by hygroscopic growth of aerosols, rather than simply by high aerosol loading. When RH was above 90%, haze aerosols started to be transformed from haze to fog. This study calls for more efforts to control emissions to prevent haze events in the region.

Key words: haze; fog; transformation; meteorological elements

CLC number: P427.2 **Document code:** A

doi: 10.16555/j.1006-8775.2016.S1.007

1 INTRODUCTION

Low visibility caused by fog or severe haze can be a heavy burden for air transport and road traffic. Pollutant particle concentrations during haze or fog events can be several times, or even a dozen times, higher than those during normal weathers, and pollutant particles in the air threaten the health of humans and other living things in many regions in the world (Jacqueline et al. ^[1]; Poschl ^[2]). Due to fast development in China in recent years, China's regional haze in urban areas has increased significantly, while there is a decreasing trend of foggy days in China (Tie et al. ^[3]; Fu et al. ^[4]). The Yangtze River Delta (YRD) has suffered from severe

pollutions caused by high concentrations of aerosol particles resulted from emissions from fossil fuel and biomass burning, transportation and other combustion sources (Chen et al. ^[5]). Concentrations of aerosol particles greatly exceeded the recently revised ambient air quality standard of China for $\text{PM}_{2.5}$ and were at least 10 times those measured in eastern US. The main cause of haze is atmospheric aerosol particles, and fog could decrease $\text{PM}_{2.5}$ and PM_{10} near the ground (Fan et al. ^[6]). Aerosols in the environment are decided by particle size, shape and chemical composition (Okada et al. ^[7]). Atmospheric fine particulates play a major role in air pollution (He et al. ^[8]).

The formation of haze is closely linked to

Received 2015-07-28; **Revised** 2016-03-15; **Accepted** 2016-07-15

Foundation item: National Natural Science Foundation of China (41275151, 41375138); Graduate Student Innovation Plan for the Universities of Jiangsu Province (CXZZ13-0514); a project funded by the Priority Academic Program Development of Jiangsu Higher Education Institutions

Biography: ZHANG Shu-ting, Ph.D. candidate, primarily undertaking research on atmospheric environment.

Corresponding author: ZHANG Shu-ting, e-mail: zhangst_10@nuist.edu.cn

meteorological and atmospheric conditions (Lai and Sequeira^[9]; Li et al.^[10]). Atmospheric haze is mainly gathered in the boundary layer, so wind, temperature and humidity below 850 hPa are the most important factors. When there is an inversion layer in the lower troposphere, the atmosphere is in a stable state, which would limit vertical dispersion of pollutants (Pilie et al.^[11]; Roach et al.^[12]). Annual variation of haze days is mainly related to aerosol pollution condition and to changes of surrounding environment. Calm condition in winter is optimal for haze to occur. High-pressure system is the main synoptic system in which haze can occur (Wang et al.^[13]). The main reason is that atmospheric stratification is stable and the inversion layer is much thicker in winter; as a result, pollutants are much easier to gather. In contrast, in weather systems of cyclone and easterly belt, haze days occur rarely.

Six Chinese megacities suffered from continuously decreasing visibility in the past 30 years (Chang et al.^[14]). The visibility trend could be attributed to the increase in sulfur dioxide emission or aerosol concentration; however, no causality could be established so far. Many in-situ measurements have already been carried out to study haze and fog under different relative humidity (RH). Results showed that low visibility events under low RH condition were mostly induced by heavy aerosol loading, while those under high RH condition were due to the influence of aerosol hygroscopic growth becoming stronger, which could lead to low visibility events even under moderate aerosol pollutants. An important source of aerosol particles is local emission (Chan and Yao^[15]). Some authors analyzed the highest level of atmospheric environment pollutants in winter resulted from vehicle exhaust and coal/coke emissions, and concluded equally important contributions of local emission and regional transport in North China, under the meteorological conditions of low temperature, low RH, weak radiation, and low boundary-layer height (Chen et al.^[16]; Chen et al.^[17]; Dai et al.^[18]).

Existing results about the effect of haze aerosols on fog are not consistent. Some studies showed that the increase of haze aerosols could strengthen fog formation and development (Jia and Guo^[19]), and others showed that the radiation effect induced by haze aerosols could lead to reduction of fog occurrence in frequency (Gautam et al.^[20]). In recent years, fog and haze events occurred frequently in the YRD region of China; however, the transition of haze to fog is not well understood. In this study, we analyzed haze-to-fog transformation during a long lasting, low visibility episode in Nanjing and characteristics of boundary layer using in-situ measurements of macro- and micro-physics on haze-to-fog days in winter 2013. The goal of this study is to analyze haze-to-fog transformation

mechanism in order to provide more scientific evidence for identification and prediction of haze and fog events. The paper is organized as follows. Section 2 describes the in-situ fog and haze measurements, introducing the observation period, site and data. In section 3.1, general information on haze to fog events is described. Sections 3.2 to 3.4 address the meteorological elements of wind, temperature and RH in one haze-to-fog event. Aerosols and cloud concentration number (CCN) concentration during haze-to-fog transition are analyzed in section 3.5. Summary and conclusion are given in section 4.

2 DATA AND METHODS

2.1 Data and site information

The YRD had been undergoing rapid development during the last three decades. Nanjing is a megacity in the YRD with high population density and a well-developed economy. Urbanization has brought great stress to local environment and haze-related disasters happened frequently. The field study focusing on physics characteristics in fog and haze was carried out in Dec. 2013. The sampling site was located at (118.7°E, 32.2°N; 22 m above the sea level) in NUIST (Nanjing University of Information and Science Technology), which is north of the Yangtze River and surrounded by various pollution sources, such as petrochemical factories, a steel plant, a thermal power station, a nitrogenous fertilizer plant, and highways (Lu et al.^[21]).

2.2 Instruments

The measurements collected during the field experiment include visibility, boundary-layer profiles and CCN number concentration, among others. Visibility and real-time weather were automatically measured and recorded every 30s with a VPF-730 Automated Present Weather Observing System (Biral, Bristol, UK). The instrument has an optical transmitter, a forward scatter receiver and a back-scatter receiver, which record fog density, precipitation identity, rain rate, and snowfall rate. The visual range of the instrument is from 10 m to 75km. The relative error of the instrument is $\pm 10\%$ for visibility less than 16km, and $\pm 20\%$ for visibility between 16 and 30km.

Detection of boundary layer was done using TP/WVP-3000 microwave radiometer (Radiometrics, USA), which detects temperature and liquid water-vapor profiles from the earth's surface to 10km. It has five oxygen channels and seven water-vapor channel. TP/WVP-3000 recorded data every minute. Brightness temperature range is 0-400K. Surface temperature detection and relative humidity precisions are 2%.

The ability of Model 3321 Aerodynamic Particle Sizer Spectrometer (APS) to make accurate mass-weighted size distribution measurement was evaluated. Sampling frequency was 1 min, and measurement particle scales were 0.37-20 μm . As a result, the APS 3321 system detected particles that were less than 0.3 μm in aerodynamic diameter using the lowest size bin.

A continuous-flow dual CCN counter (CCN-200) manufactured by Droplet Measurement Technologies (DMT, USA) was utilized to measure CCN concentrations at different supersaturation values (Roberts and Nenes^[22]; Lance et al.^[23]). Five supersaturation values (nominally 0.1, 0.2, 0.4, 0.8, and 1.0%) made up a cycle of half an hour, taking 10 min for 0.1% and 5 min for the other supersaturation values. Cloud room total airflow rate was 500 $\text{cm}^3 \text{min}^{-1}$, ratio of best sheath flow and sampling airflow rate was 10:1, sampling frequency was 1 Hz, and measurement particle scales were 0.75-10.00 μm (Li et al.^[24]).

Surface meteorological conditions and synoptic weather data were obtained from the China Meteorological Administration's comprehensive observation network. Water-vapor divergence was obtained using the Final Analysis Data (FNL) from the National Centers for Environmental Prediction (NCEP) of the US.

3 RESULTS

3.1 General information on haze to fog transformation

Atmospheric conditions may be classified into

three regimes according to visibility: clear sky, fog and haze. Classification is usually done based on absolute values of visibility range (Tardif and Rasmussen^[25]). Clear-sky regime is defined arbitrarily for visibility better than 5 000 m, in contrast to hazy and foggy conditions when visibility can reach dramatically lower values. The international definition of fog is an observed horizontal visibility below 1 km in the presence of suspended water droplets and/or ice crystals (National Oceanic and Atmospheric Administration, 1995). Haze regime occurs as a transition between clear-sky and fog regimes, and visibility is highly variable in haze regime. Haze regime is defined as visibility lower than 5 000 m until fog occurs (Elias et al.^[26]). Haze transition phase is defined by the start of an aerosol activation process. Computation for haze is done for visibility lower than 2 000 m, as droplets appear at visibility between 1 400 and 2 000 m. The visibility values of 400 and 880 m characterize the transition phase between fog and haze regimes, which is consistent with the 500-1 000 m visibility interval corrected. In our study, we use RH and visibility (Vis) to define fog and haze (Fig. 1): it is fog if $\text{Vis} < 1 \text{ km}$ and $\text{RH} \geq 90\%$; it is haze, if $\text{Vis} < 5 \text{ km}$ and $\text{RH} < 80\%$; it is the transition phase, if $\text{Vis} < 1 \text{ km}$ and $80\% < \text{RH} < 90\%$; and it is clear-sky regime if visibility value is better than 5 000 m. The haze-to-fog transition during our survey can be roughly divided into four stages (Table 1): haze stage (2340 LST (LST=UTC+8h) 3 December to 1047 LST 4 December), haze-to-fog stage (2321 LST 4 December to 1026 LST 5 December), fog stage I (2344 LST 5 December to 0820 LST 6 December), and fog stage II (2125 LST 6 December to 0932 LST 9 December).

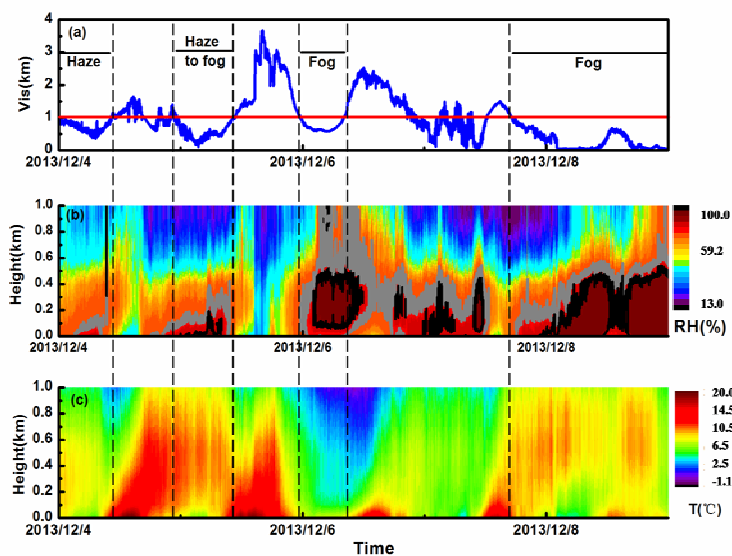


Figure 1. Temporal variations of (a) visibility, (b) RH and (c) temperature. Black line is $\text{RH}=90\%$, and gray line is $\text{RH}=80\%$.

3.2 Impact of surface wind on haze-to-fog transformation

Wind speed and boundary-layer stratification provide the weather background for haze or fog events. At surface, the weak pressure system

controlled most areas of central and eastern China, and the dominant flows were from the southwest and west, with wind speed less than 3 m s^{-1} , which could result in a haze-fog episode (Yang et al.^[27]). Early studies on the formation and evolution mechanisms of haze events in Beijing and found the primary reasons were stable anti-cyclonic circulation at surface, lowering of planetary boundary-layer height (Deng et al.^[28]). Wang et al found that the cold air belonged to the horizontal through turning to longitudinal style, the ground was controlled by the pre-high anticyclone and the ground front zone had been pressed to the Jiangnan region^[14]. Zhang et al showed that the East Asian winter monsoon was weak in January 2013, an abnormally high pressure center occurred at 42.5°N , 120.0°E , and the cold air of post through was difficult to invade eastern China as a result^[29]. Fig. 2 is the weather pattern over eastern China from 0800 LST 4 December to 0932 LST 9 December 2013. At high altitude, a trough in the north moved eastward on 3 December, and moved away from Jiangsu Province at 2000 LST 4 December. On 5 December, the East Asian major trough moved eastward, while the mid-latitude geopotential height field appeared to be zonally oriented. Until 2000 LST 8 December, an upper-layer trough combined with the mid-lower layer cold air shear moved eastward, bringing cold air southward near the surface, which impacted the weather in Nanjing. According to the surface observation, the northwesterly prevailed in Nanjing on 3 December, since the city was in front of a weak high-pressure system that was centered in North China. On 4 December, the weak cold air moved southward and caused pressure gradient to decrease. Nanjing was under the control of homogeneous pressure, and the wind speed was reduced. Severe cold air intruded southward since the night of 8 December, which caused pressure gradient to increase, and wind speed increased to $6\text{--}8 \text{ m s}^{-1}$. The visibility obviously improved at 1700 LST 9 December, and the large-scale haze-to-fog episode came to an end.

Wind direction can influence the transport of pollutants, while wind speed greatly influences atmospheric dispersion capability. Low wind speed in the horizontal direction implies that the atmosphere is rather stable, and that the dispersion of local emissions is limited. Air-mass transport can bring in pollutants or clean air from distant, influencing local concentrations of particles.

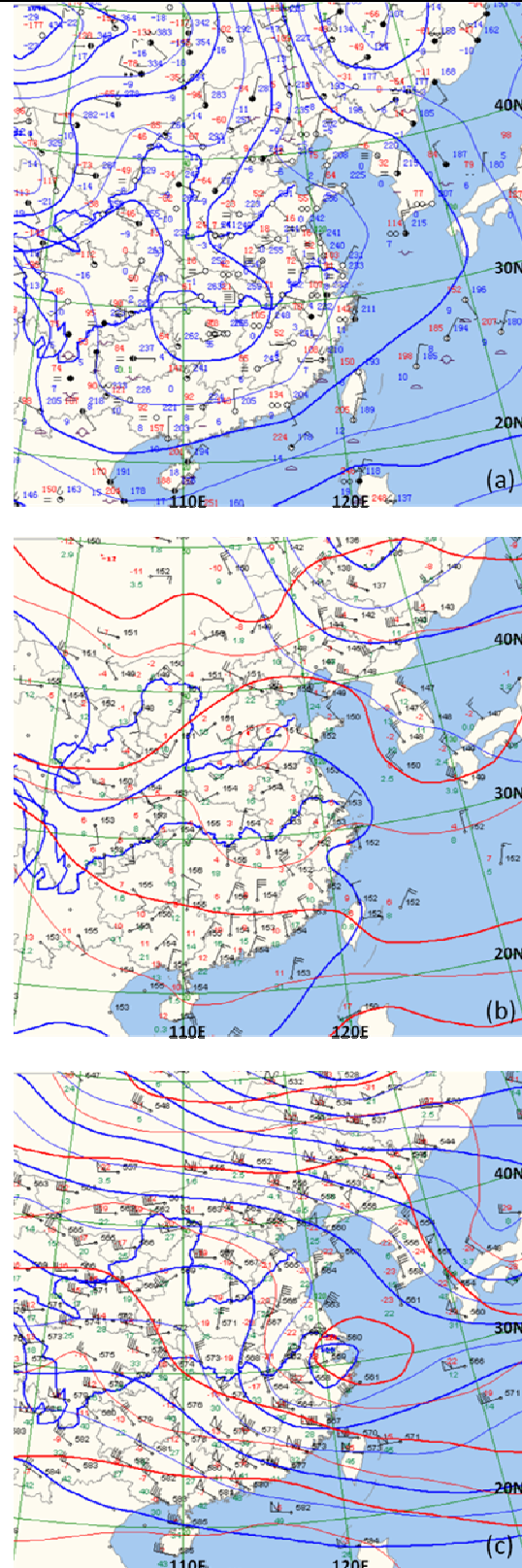


Figure 2. Average synoptic weather during the haze-to-fog process of 4-9 December 2013. (a) Surface wind field; (b) geopotential height field at 850 hPa; (c) geopotential height field at 500 hPa.

Figure 3 shows the wind speed was less than 1 m s^{-1} in the haze event, which helped to maintain the stable boundary layer near the surface. Surface

roughness also influences wind speed. Cities with densely distributed tall buildings have high surface roughness, which slows down near-surface wind. Low wind speed indicates that dispersion had been weakened over the observation region. In Fig. 3, in the northwest to southwest by west (NW-WSW) the wind speed (WS) was high before haze transformed to fog, and the concentration of aerosol and CCN showed a relatively high level. According to HYSPLIT back trajectories and fire hot spots for the haze-fog periods during the observation. Zhang Xiangzhi, the deputy director of Testing center of Department of Environmental Protection, said “The concentrations of potassium ion and black carbon in the air were increased. These two compositions were 0.5 times higher than normal. This is caused by straw burning! These kinds of particles mainly came from the north of Jiangsu province.” The winds from these directions brought in pollutants from straw combustion; so, we could conclude the polluted air masses from western areas contributed to the

accumulation of particles in Nanjing (Fig.4). When the wind speed slowed down, the haze began to transform into fog. Local emission accompanied by regional transport from west was responsible for the particles in haze-to-fog transition. Fig. 5a shows the spatial distribution of surface wind direction during the haze event. The site was controlled by the northeasterly wind, which transported the pollutants from the north to the site, while the southwest part of the observation site was dominated by wind from the northwest in the haze event. An inverse relationship between concentration and wind speed suggests the predominance of local sources, because strong wind sent pollutants out of the study area whereas weak wind allowed pollutants to accumulate over time. Apart from local emission, regional transport was reported as an important cause for particle concentration in the atmospheric environment (Peter et al.^[30]). The weak northerly wind led to the accumulation of aerosols and their precursors around the site (Xu et al.^[31]; Gao et al.^[32]).

Table 1. Starting time, ending time, duration, means and standard deviations (in parenthesis) of key properties under different weather conditions in 2013.

Regime	Time period		Time duration	Average Temp. (°C)	Average RH(%)	Average Vis (km)	Accumulation particle number concentration (cm ⁻³)	Coarse particle number concentration (cm ⁻³)
	Starting time	Ending time						
Haze	2013/12/3 23:40	2013/12/4 10:47	11h	5.6 (2.0)	73.9 (4.9)	0.7 (0.1)	348.2-15489. 2	534.4-4634.1
Haze to fog	2013/12/4 23:21	2013/12/5 10:26	11h	6.6 (1.8)	84.5 (5.1)	0.5 (0.2)	274.6-21528. 9	459.4-85238. 7
Fog I	2013/12/5 23:44	2013/12/6 8:20	9h	5.833 (0.5)	91.9 (5.4)	0.7 (0.1)	225.7-11186. 6	125.9-1314.7
Fog II	2013/12/7 17:10	2013/12/9 9:32	33h	5.879 (1.6)	94.3 (6.9)	0.3 (0.2)	270.7-152459 .8	153.4-94142. 3

Fog formation requires a favorable weather condition, say a saturated water-vapor environment. During the haze-to-fog transition, surface wind speed was low, the same as in the haze event, which is conducive to accumulation of particulate matters and their interaction with water vapor. Low surface-wind speed also provided the condition for the transformation. For wind direction, Fig. 5b shows the surface wind all came from the south and converged at the site, which transported warm and humid air to the site. There was a convergence line near 118°E. To the west of the convergence line, the near-surface wind was dominated by the southwesterly; to the east to the convergence line, the near-surface wind was the southeasterly. The southeasterly and southwesterly are the most typical carriers for water vapor to reach Nanjing. Accumulation of water vapor in the

convergence zone helped fog formation in this area.

Wind speed in the fog event was greater than that in haze and haze-to-fog transition. When fog was in development and mature stages, microphysical processes such as condensation and evaporation developed well. When the air became saturated, small perturbations could cause other physical quantities (e.g., water vapor, turbulence, or temperature) to make corresponding adjustments to achieve a new equilibrium state. In this balanced state, turbulence could develop; so, variability of wind speed would be larger than in the haze event.

Figure 5c shows the wind field in the first fog event. This fog lasted nine hours. To the north of the site, the near-surface wind was the northeasterly; to the south of the site, the wind was dominated by the northwesterly. Low-pressure rear airflow increased

convergence, so water vapor condensed and formed fog. The second fog event lasted 60 hours, but not continuously. It was dominated by the southerly wind (Fig. 5d). Near the observation site, there was the

convergence zone, and the southeasterly wind brought warm and humid air, which provided moisture for the fog to persist.

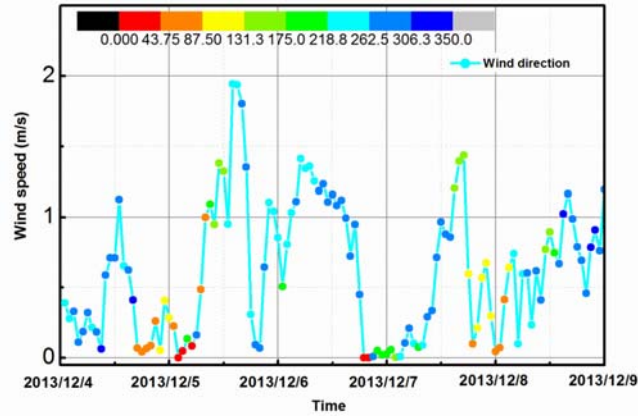


Figure 3. Temporal variations of wind speed and wind direction.

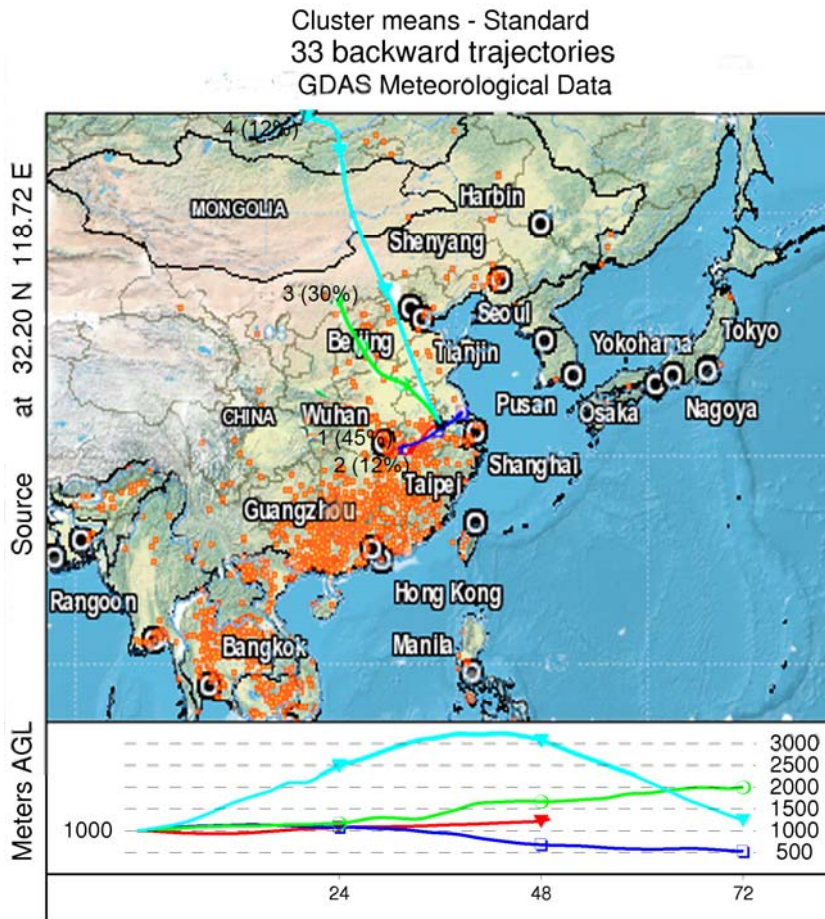


Figure 4. Back trajectory to Nanjing 72h and fire hot spots on YRD during 1-15 December 2013, the interval between two points is 12h, and the star point is Nanjing.

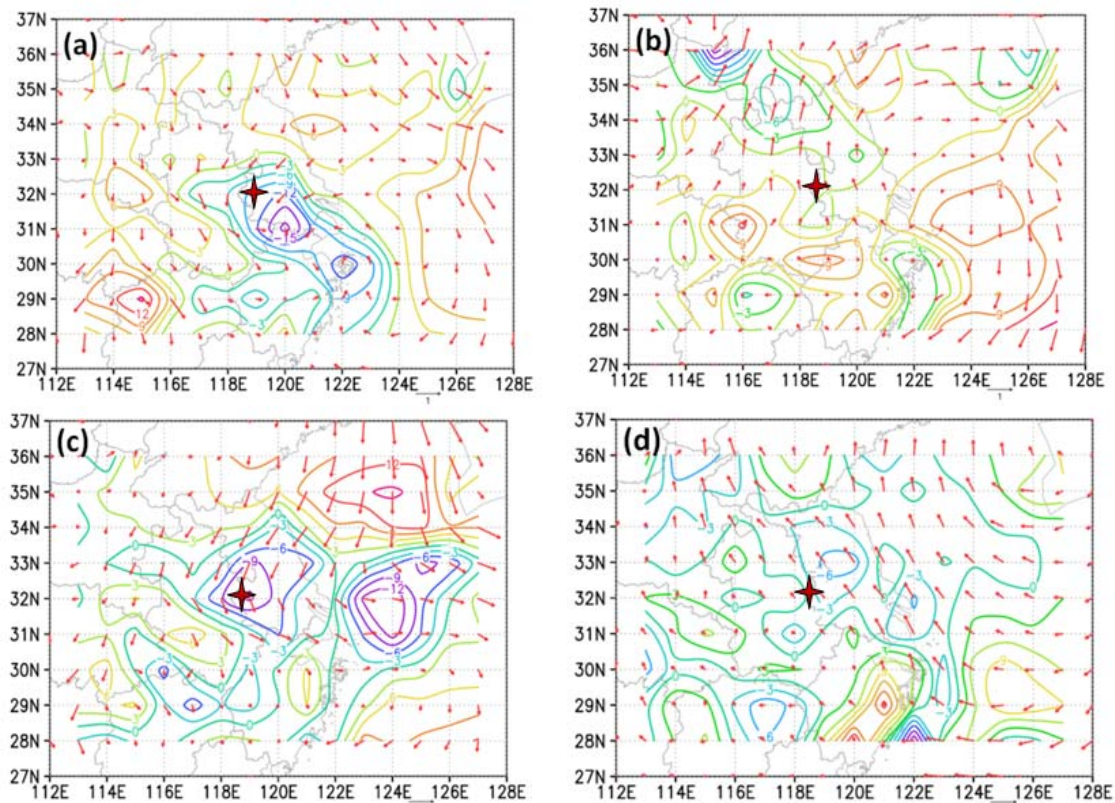


Figure 5. Vapor flux divergence ($\text{g}/(\text{hPa}\cdot\text{cm}^2\cdot\text{s})$) and wind field (m/s) on the ground: (a) 0000 LST 4 December 2013, (b) 0000 LST 5 December 2013, (c) 0000 LST 6 December 2013, and (d) 0000 LST 8 December 2013. The star is the observation site.

3.3 Impact of temperature on haze-to-fog transformation

There was an inversion layer near the surface before the formation of fog (Niu et al.^[33]), and the fog formed in the inversion layer. After the formation of the fog, the inversion layer gradually moved to the top of the fog. In the development stage of the fog, temperature decreased at the moist adiabatic lapse rate. A temperature inversion is a stable stratification and will accumulate moisture and energy in the inversion layer; so, temperature inversion provides a condition for changing size and chemical reaction of particles.

Figure 6 shows the profiles of temperature during the haze-to-fog transformation. The highest surface temperature appeared during the haze event, followed by that in the haze-to-fog transition, and the lowest surface temperature was in the fog event. Low temperature is generally favorable for moisture condensation, because it will make more particles hygroscopic for activation and growth. The haze-to-fog transition happened basically in the inversion layer. The height of the temperature inversion was about 400 m. When there was a temperature inversion in haze, the inversion intensity was weak and the temperature-difference was $4^\circ\text{C}/\text{km}$ or less. In the haze event the temperature was higher than that during the transition and the fog days at

surface, there was less water vapor, aerosol condensation was weak, release latent heat was small.

In the haze-to-fog transition, the intensity of the inversion was stronger, and temperature-difference was about 6°C km^{-1} , approaching the inversion layer intensity in the fog event. During the haze-to-fog transition, the thickness of the inversion layer increased, the boundary layer was stable and the water vapor accumulated at night.

Fog developed in the inversion layer. The intensity of inversion was also the maximum in the fog event, though the temperature inversion disappeared sometimes in the fog event. This suggests that fog event could occur in unstable temperature stratification. The two fog events were slightly different. In the first fog event, since there was the northerly wind, an isothermal layer began to appear between 100 and 200 m, and then fog extended to the ground at this location. In the second fog event, water-vapor transport from the south was one of the important factors for transition from haze to fog. Temperature at the inversion layer top was significantly higher in the fog event than in the haze event; this was due to the fact that the fog in the development stage released latent heat, inverse radiation hindered longwave radiative cooling near the surface, and warm advection was also an important reason for the inversion at the fog top.

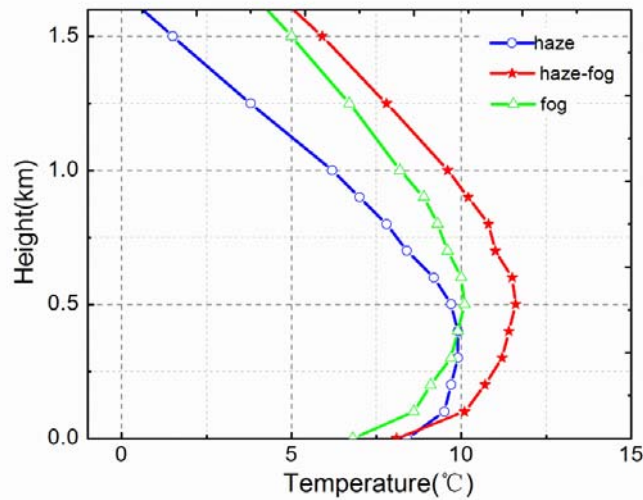


Figure 6. Temperature profiles during the haze-to-fog transformation process.

3.4 Impact of RH on haze-to-fog transformation

Ambient RH can influence haze or fog formation, development and dissipation by affecting hygroscopic growth of atmospheric aerosols. Under the same particle concentration, the higher the RH is, the lower the visibility becomes. During the haze event, the main features were accumulation of aerosols, low RH near the surface and low wind speed. Mixture and transition of particles and water vapor usually happen under higher humidity than haze event. When the air was saturated, haze aerosols could be activated to form CCN, and the aerosol particles that were continuously accumulated could mix and coexist with fog droplets, thereby promoting an explosive development of fog event.

Figure 6 shows the water-vapor divergence in the ground layer. During the haze event, the site was in a region of water-vapor divergence (negative center), suggesting that moisture converged in Nanjing area. Particles began hygroscopic growth; but due to high concentration of hygroscopic particles and weak water-vapor divergence, particles could not grow into fog droplets. However, this could serve as preparation period of fog, namely, continued moisture convergence and water-vapor transport could turn haze into fog. Lack of moisture, haze would remain as haze; with cold air coming down, haze would dissipate.

During the haze-to-fog transition, although there was no obvious moisture convergence near the observation site, the dominant wind direction south of the site would bring warm and humid air from the south, increasing air humidity. Hygroscopic growth continued, and the haze could transform into fog. Another possible reason was that air pollution had become more complex over the years, and secondary

aerosol hygroscopic was stronger and more inclined to moisture absorption and growth leading to reduced visibility. This means a higher fraction of haze events was caused by hygroscopic growth of aerosols. The reduction in primary aerosol emission further amplified this effect, and RH also had obvious and important effect on the scale, size and number of air pollutants.

3.5 Haze aerosol characteristics and activation ratio during the haze-to-fog transformation

Table 1 shows the minimum values of accumulation particle number concentration were smaller than coarse-particle number concentration in non-fog days, and vice versa. The maximum values of accumulation particle number concentration were all larger than coarse-particle number concentration, except during the transition from haze to fog. The coagulation of haze aerosols happened at size below $0.5\mu\text{m}$ (Husar and Holloway^[34]); in particular, the reduction of aerosol particles less than $0.2\mu\text{m}$ during the transition from haze to fog was caused primarily by coagulation (Jacqueline^[11]). In the haze-to-fog transition during which air was saturated, some aerosols in accumulation mode could be activated as CCN and converted to fog droplets through condensation growth. Table 2 shows that temporal variations of aerosol number concentration, accumulation number concentration, coarse-particle number concentration, and CCN concentration. Nccn (CCN number concentration) value depended strongly on weather systems during the measurement period. High Nccn values were observed during periods of heavy aerosol pollution. Nccn was found to be as high as 38198.4 cm^{-3} at 0.99% supersaturation. Normally, Nccn was about 5929.1 and 9967.9 cm^{-3} at supersaturation of 0.198% and 0.397%, respectively,

and more than 30000.0 cm^{-3} at supersaturation above 0.5%. Under different weathers, CCN concentrations were different. On the haze-to-fog days, the CCN

concentration was the highest, followed by that on the fog days.

Table 2. Statistics of CCN Number Concentration. The $N_{ccn} (\text{cm}^{-3})$ at five supersaturations are presented. The minimum, maximum, mean value and the corresponding standard deviation are presented. The last line is the number of samples.

SS	0.198%	0.397%	0.596%	0.79%	0.99%
Min	1.6	153.8	4 692.3	5 173.5	5 304.1
Max	11 770.4	25 546	33 797.4	36 533.3	38 198.4
Mean	5 929.1	9 967.9	11 387.6	12 187.6	12 262.8
Std	1 958.9	3 953.1	4 703.2	5 104.4	5 133.4
N	431	502	503	501	415

In an attempt to analyze activation of aerosols to CCN and the conversion of CCN to fog droplets, the ratios of activation based on the observed number concentration of aerosols and CCN (N_{cn} (aerosol number concentration) and N_{ccn}) are calculated. The ratio for aerosol activation to CCN is denoted by activation ratio:

$$\text{Activation ratio} = N_{ccn}/N_{cn} \times 100\%, \quad (1)$$

Figure 7 shows the activation ratios at supersaturation of 0.596%, 0.79% and 0.99%. Aerosols with size less than $15 \mu\text{m}$ were too small to activate under the three supersaturation values, while particles of $35 \mu\text{m}$ had the activation ratio of 0.9 at all three supersaturation values. Most particles of $25 \mu\text{m}$ were activated, because small soluble fraction was unable to be activated. The activation ratio strongly depends on particle size: the activation ratio increases with increasing diameter. When RH was above 90%, haze aerosols started to be transformed from haze to fog. The release of latent heat produced high number concentration of haze particles intensified Brownian

coagulation and caused the size of aerosols to shift from smaller size to larger one, and provided appropriate sizes of aerosols, which can be effectively activated to CCN. Under strong cooling and high humid conditions, the explosive activation of CCN enhanced the mixture and development of haze to fog.

Figure 8 shows the temporal variation of aerosol size distribution during transition. Corresponding with the temporal variation of relative humidity in Fig. 1, we could see the spectrum of aerosol during 00:00 to 09:00 on December 6. Relative humidity was high, and maintained a long time, aerosol particles hygroscopic growth, large particle number concentration gradually increased, until 08:00 in the morning, aerosol particle number concentration could reach $13.95 \text{ cm}^{-3} \mu\text{m}^{-1}$ when aerosol particle diameter was greater than $0.5 \mu\text{m}$. The spectral of aerosol particles moved to the large particles step by step. This showed that the relative humidity had significant effect to aerosol hygroscopic in the process of condensation.

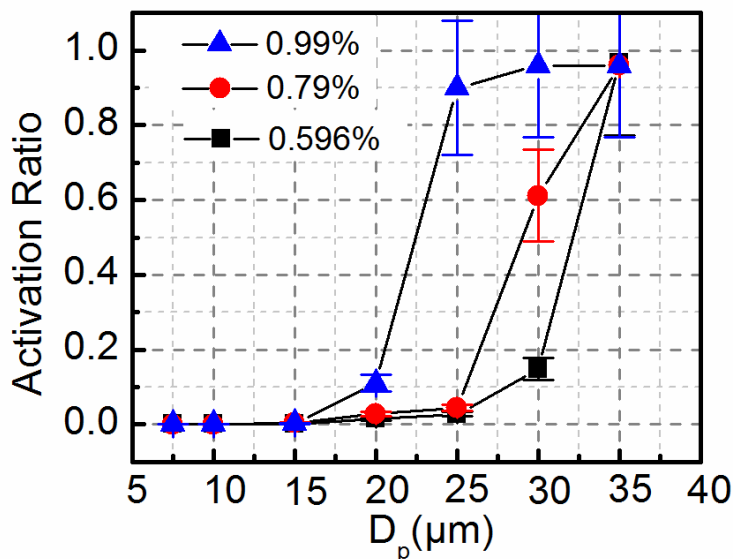


Figure 7. Average activation curves of ambient aerosols.

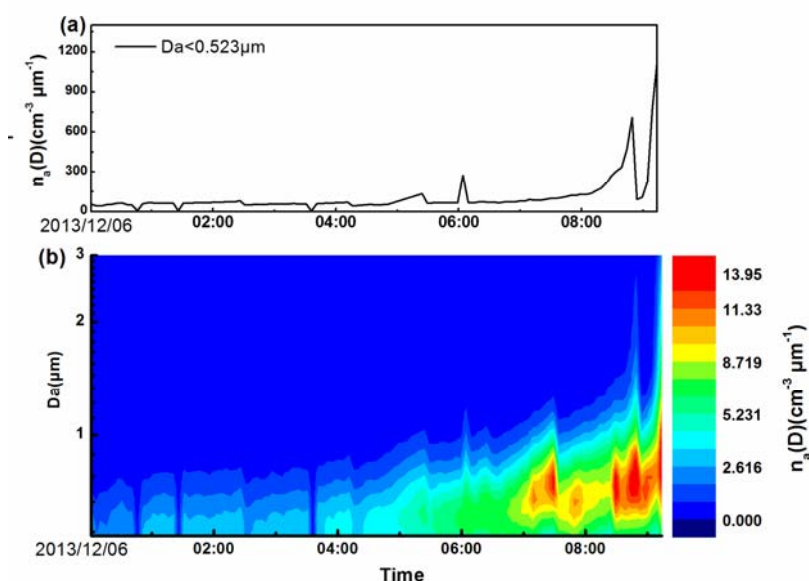


Figure 8. The temporal variation of aerosol size distribution during transition.

4 CONCLUDING REMARKS

An unusual haze-to-fog transition occurred during 4-9 December 2013. The low visibility (<1 km) lasted five days, which was captured by a field campaign. The measurements included visibility, common meteorological variables, particle number concentration, and planetary boundary-layer structure. This paper focused on the major properties of the haze-to-fog transition, and the relationship between haze and fog.

Our conclusions are as follows:

(1) At high altitude, the East Asian trough moved eastward and was controlled by mid-latitude geo-potential height field that appeared zonally over the YRD region. An upper-layer trough and the mid-lower layer cold air shear moved eastward, causing cold air to intrude southward near the surface. According to the surface observations, Nanjing was in front of a weak high-pressure system that was centered in North China and was controlled by homogeneous pressure; as a result, the wind speed was reduced. This weather system led to a lower surface wind speed and stably stratified atmosphere.

(2) Wind speed was less than 1 m s^{-1} in the haze event, and the site was under the northerly wind, which transported pollutants from the north to the site. During the haze-to-fog transition, the surface wind all came from the south and converged at the observation site, which transported warm and humid air to the site. The variability of wind speed during the fog event was larger than that during the haze event. Low-pressure rear airflow increased convergence of water vapor.

(3) The highest surface temperature appeared in

the haze event, followed by that in the haze-to-fog transition, and the lowest surface temperature appeared in the fog event. In the haze event, the inversion intensity was weak. In the fog event, the inversion intensity was the strongest, but the temperature inversion disappeared sometimes during the fog event. This suggests that fog event can occur under unstable temperature stratification. The temperature of the inversion layer top was significantly higher in the fog event than in the haze event. The development of fog may be explained by surface radiation cooling and associated latent-heat release.

(4) The minimum values of accumulation particle number concentration were smaller than coarse-particle number concentration in non-fog days, and vice versa. The maximum values of accumulation particle number concentration were all larger than coarse-particle number concentration except in the transition from haze to fog. Nccn depended strongly on weather system during the measurement period. When RH was above 90%, haze aerosols started to be transformed from haze to fog. The release of latent heat caused the size of aerosols to shift from smaller size to larger one, and provided appropriate size aerosols that can be effectively activated to CCN. Under strong cooling and high humidity conditions, the explosive activation of CCN enhanced the mixture of particles and water vapor, and developed of haze and fog.

REFERENCES:

[1] JACQUELINE D C, ANDREW J G, JAMES M S, et al. Cytokine production by human airway epithelial cells after exposure to an air pollution particle is metal-dependent [J].

- Toxicol Appl Pharmac, 1997, 146(1997): 180-188.
- [2] POSCHL U. Atmospheric aerosols: composition, transformation, climate and health effects [J]. *Agenwandte Chemie Int Ed*, 2005, 44(46): 7 520-7 540.
- [3] TIE Xue-xi, BRASSEUR G P, ZHAO Chun-sheng, et al. Chemical characterization of air pollution in Eastern China and the Eastern United States [J]. *Atmos Environ*, 2006, 40: 2 607-2 625.
- [4] FU Qing-yan, ZHUANG Guo-shun, WANG Jing, et al. Mechanism of formation of the heaviest pollution episode ever recorded in the Yangtze River Delta, China [J]. *Atmos Environ*, 2008, 42: 2 023-2 036.
- [5] CHEN J, ZHAO C S, MA N, et al. A parameterization of low visibilities for hazy days in the North China Plain [J]. *Atmos Chem Phys*, 2012, 12: 4 935-4 950.
- [6] FAN S X, HUANG H L, FAN T, et al. Size distribution characteristics of polycyclic aromatic hydrocarbons of PM10 in foggy days in the north suburb of Nanjing [J]. *Environ Sci*, 2009, 30(9): 2 707-2 715.
- [7] OKADA K M, IKEGAMI, ZAIZEN Y. The mixture state of individual aerosol particles in the 1997 Indonesian haze episode [J]. *J Aerosol Sci*, 2001, 32(11): 1 269-1 279.
- [8] HE Jia-bao, FAN Shu-xian, MENG Qing-zi, et al. Polycyclic aromatic hydrocarbons (PAHs) associated with fine particulate matters in Nanjing, China: Distributions, sources and meteorological influences [J]. *Atmos Environ*, 2014, 89(2014): 207-215.
- [9] LAI L Y, SEQUEIRA Y R. Visibility degradation across Hong Kong: its components and their relative contributions [J]. *Atmos Environ*, 2001, 35(34): 5 861-5 872.
- [10] LI Z Q, Gu X, WANG L, et al. Aerosol physical and chemical properties retrieved from ground-based remote sensing measurements during heavy haze days in Beijing winter [J]. *Atmos Chem Phys Discuss*, 2013, 13(2): 5 091-5 122.
- [11] PILIE R J, MACK E J, KOCMOND W C, et al. The life cycle of valley fog. Part I: Micrometeorological characteristics [J]. *J Appl Meteorol*, 1975, 14(1975): 347-364.
- [12] ROACH W T, BROWN R, CAUGHEY S J, et al. Readings. The physics of radiation fog: I- a field study [J]. *Quart J Roy Meteorol Soc*, 1976, 102: 313-333.
- [13] WANG Hong-lei, AN Jun-lin, SHEN Li-juan, et al. Mechanism for the formation and microphysical characteristics of submicron aerosol during heavy haze pollution episode in the Yangtze River Delta, China [J]. *Sci Total Environ*, 2014, 490(2014): 501-508.
- [14] CHANG Di, SONG Yu, and LIU Bing. Visibility trends in six megacities in China 1973-2007 [J]. *Atmos Res*, 2009, 94: 161-167.
- [15] CHAN C K, Yao Xiaohong. Air pollution in mega cities in China [J]. *Atmos Environ*, 2008, 42(1): 1-42.
- [16] CHEN Xun-lai, FENG Ye-rong, WANG An-yu, et al. Numerical experiment research on air pollutants during atmospheric haze over the multi-cities of Pearl River Delta region [J]. *Acta Sci Nat Univ Sunyatseni*, 2007, 46(4): 103-107 (in Chinese).
- [17] CHEN Y, ZHAO C, ZHANG Q, et al. Aircraft study of mountain chimney effect of Beijing, China [J]. *J Geophys Res*, 2009, 114: D08306.
- [18] DAI Yong-li, TAO Jun, LIN Ze-jian, et al. Characteristics of haze and its impact factors in four megacities in China during 2006-2009 [J]. *Environ Sci*, 2013, 34(8): 2 925-2 933.
- [19] JIA Xing-can, GUO Xue-liang. Impacts of anthropogenic atmospheric pollutant on formation and development of a winter heavy fog event [J]. *China J Atmos Sci*, 2012, 36: 995-1 008 (in Chinese).
- [20] GAUTAM R, HSU N C, KAFATOS M, et al. Influences of winter haze on fog/low cloud over the Indo-Gangetic [J]. *J Geophys Res*, 2007, 112: 207-218.
- [21] LU Chun-song, NIU Sheng-jie, TANG Li-li, et al. Chemical composition of fog water in Nanjing area of China and its related fog microphysics [J]. *Atmos Res*, 2010, 97(2010): 47-69.
- [22] ROBERTS G C, NENES A. A continuous-flow streamwise thermal-gradient CCN chamber for atmospheric measurements [J]. *Aerosol Sci Tech*, 2005, 39: 206-221.
- [23] LANCE S, SMITH J, NENES A. Mapping the operation of the DMT continuous flow CCN counter [J]. *Aerosol Sci Tech*, 2006, 40: 242-254.
- [24] LI Li, YIN Yan, GU Xue-song, et al. Observational study of cloud condensation nuclei properties at various altitudes of Huangshan Mountains [J]. *Chin J Atmos Sci*, 2014, 38(3): 410-420.
- [25] TARDIF R, RASMUSSEN R M. Event-based climatology and typology of fog in the New York city region [J]. *J Appl Meteor Climatol*, 2007, 46: 1 141-1 168.
- [26] ELIAS T, HAEFFELIN M, DROBINSKI P, et al. Particulate contribution to extinction of visible radiation: Pollution, haze, and fog [J]. *Atmos Res*, 2009, 92: 443-454.
- [27] YANG Xin, CHEN Yi-zhen, LIU Hou-feng, et al. Characteristics and formation mechanism of a winter haze-fog episode in Tianjin, China [J]. *Atmos Environ* 2014, 98(2014): 323-330.
- [28] DENG Z Z, ZHAO C S, MA N, et al. An examination of parameterizations for the CCN number concentration based on in situ measurements of aerosol activation properties in the North China Plain [J]. *Atmos Chem Phys*, 2013, 13: 6 227-6 237.
- [29] ZHANG J K, SUN Y, LIU Z R, et al. Characterization of submicron aerosols during a serious pollution month in Beijing (2013) using an aerodyne high-resolution aerosol mass spectrometer [J]. *Atmos Chem Phys Discuss*, 2013, 13(7): 19 009-19 049.
- [30] PETER K K, JOHN G W, JUDITH C C, et al. Aleis. Seasonal characteristics and regional transport of PM2.5 in Hong Kong [J]. *Atmos Environ*, 2005, 39(2005): 1 695-1 710.
- [31] XU Feng, NIU Sheng-jie, ZHANG Yu, et al. Analyses on chemical characteristic of spring sea fog water on Donghai Island in Zhanjiang, China [J]. *China Environ Sci*, 2011, 31(3): 353-360.
- [32] GAO Jian, WANG Tao, ZHOU Xue-hua, et al. Measurement of aerosol number size distributions in the Yangtze River delta in China: formation and growth of particles under polluted conditions [J]. *Atmos Environ*, 2009, 43: 829-836.
- [33] NIU Sheng-jie, LU Chun-song, Yu Hua-ying, et al. Fog research in China: an overview [J]. *Adv Atmos Sci*, 2010, 27(3): 639-662.
- [34] HUSAR R B, HOLLOWAY J M. The properties and climate of atmospheric haze [J]. *Hygroscopic Aerosols*, Hampton Virginia, A Deepak Publishing, 1984: 129-170.

Citation: ZHANG Shu-ting and NIU Sheng-jie. Haze-to-fog transformation during a long lasting, low visibility episode in Nanjing [J]. *J Trop Meteorol*, 2016, 22(S1): 67-77.